

Measurement of the Cross Section for $e^+e^- \rightarrow \Xi^- \bar{\Xi}^+$ and Observation of an Excited Ξ Baryon

M. Ablikim,¹ M. N. Achasov,^{10,d} P. Adlarson,⁵⁹ S. Ahmed,¹⁵ M. Albrecht,⁴ M. Alekseev,^{58a,58c} A. Amoroso,^{58a,58c} F. F. An,¹ Q. An,^{55,43} Y. Bai,⁴² O. Bakina,²⁷ R. Baldini Ferroli,^{23a} I. Balossino,^{24a} Y. Ban,^{35,1} K. Begzsuren,²⁵ J. V. Bennett,⁵ N. Berger,²⁶ M. Bertani,^{23a} D. Bettoni,^{24a} F. Bianchi,^{58a,58c} J. Biernat,⁵⁹ J. Bloms,⁵² I. Boyko,²⁷ R. A. Briere,⁵ H. Cai,⁶⁰ X. Cai,^{1,43} A. Calcaterra,^{23a} G. F. Cao,^{1,47} N. Cao,^{1,47} S. A. Cetin,^{46b} J. Chai,^{58c} J. F. Chang,^{1,43} W. L. Chang,^{1,47} G. Chelkov,^{27,b,c} D. Y. Chen,⁶ G. Chen,¹ H. S. Chen,^{1,47} J. C. Chen,¹ M. L. Chen,^{1,43} S. J. Chen,³³ Y. B. Chen,^{1,43} W. Cheng,^{58c} G. Cibinetto,^{24a} F. Cossio,^{58c} X. F. Cui,³⁴ H. L. Dai,^{1,43} J. P. Dai,^{1,43} X. C. Dai,^{1,47} A. Dbeysy,¹⁵ D. Dedovich,²⁷ Z. Y. Deng,¹ A. Denig,²⁶ I. Denysenko,²⁷ M. Destefanis,^{58a,58c} F. De Mori,^{58a,58c} Y. Ding,³¹ C. Dong,³⁴ J. Dong,^{1,43} L. Y. Dong,^{1,47} M. Y. Dong,^{1,43,47} Z. L. Dou,³³ S. X. Du,⁶³ J. Z. Fan,⁴⁵ J. Fang,^{1,43} S. S. Fang,^{1,47} Y. Fang,¹ R. Farinelli,^{24a,24b} L. Fava,^{58b,58c} F. Feldbauer,⁴ G. Felici,^{23a} C. Q. Feng,^{55,43} M. Fritsch,⁴ C. D. Fu,¹ Y. Fu,¹ Q. Gao,¹ X. L. Gao,^{55,43} Y. Gao,⁵⁶ Y. Gao,⁴⁵ Y. G. Gao,⁶ Z. Gao,^{55,43} B. Garillon,²⁶ I. Garzia,^{24a} E. M. Gersabeck,⁵⁰ A. Gilman,⁵¹ K. Goetzen,¹¹ L. Gong,³⁴ W. X. Gong,^{1,43} W. Gradl,²⁶ M. Greco,^{58a,58c} L. M. Gu,³³ M. H. Gu,^{1,43} S. Gu,² Y. T. Gu,¹³ A. Q. Guo,²² L. B. Guo,³² R. P. Guo,³⁶ Y. P. Guo,²⁶ A. Guskov,²⁷ S. Han,⁶⁰ X. Q. Hao,¹⁶ F. A. Harris,⁴⁸ K. L. He,^{1,47} F. H. Heinsius,⁴ T. Held,⁴ Y. K. Heng,^{1,43,47} M. Himmelreich,^{11,g} Y. R. Hou,⁴⁷ Z. L. Hou,¹ H. M. Hu,^{1,47} J. F. Hu,^{38,h} T. Hu,^{1,43,47} Y. Hu,¹ G. S. Huang,^{55,43} J. S. Huang,¹⁶ X. T. Huang,³⁷ X. Z. Huang,³³ N. Huesken,⁵² T. Hussain,⁵⁷ W. Ikegami Andersson,⁵⁹ W. Imoehl,²² M. Irshad,^{55,43} Q. Ji,¹ Q. P. Ji,¹⁶ X. B. Ji,^{1,47} X. L. Ji,^{1,43} H. L. Jiang,³⁷ X. S. Jiang,^{1,43,47} X. Y. Jiang,³⁴ J. B. Jiao,³⁷ Z. Jiao,¹⁸ D. P. Jin,^{1,43,47} S. Jin,³³ Y. Jin,⁴⁹ T. Johansson,⁵⁹ N. Kalantar-Nayestanaki,²⁹ X. S. Kang,³¹ R. Kappert,²⁹ M. Kavatsyuk,²⁹ B. C. Ke,¹ I. K. Keshk,⁴ A. Khoukaz,⁵² P. Kiese,²⁶ R. Kiuchi,¹ R. Kliemt,¹¹ L. Koch,²⁸ O. B. Kolcu,^{46b,f} B. Kopf,⁴ M. Kuemmel,⁴ M. Kuessner,⁴ A. Kupsc,⁵⁹ M. Kurth,¹ M. G. Kurth,^{1,47} W. Kühn,²⁸ J. S. Lange,²⁸ P. Larin,¹⁵ L. Lavezzi,^{58c} H. Leithoff,²⁶ T. Lenz,²⁶ C. Li,⁵⁹ Cheng Li,^{55,43} D. M. Li,⁶³ F. Li,^{1,43} F. Y. Li,^{35,1} G. Li,¹ H. B. Li,^{1,47} H. J. Li,^{9,j} J. C. Li,¹ J. W. Li,⁴¹ Ke Li,¹ L. K. Li,¹ Lei Li,³ P. L. Li,^{55,43} P. R. Li,³⁰ Q. Y. Li,³⁷ W. D. Li,^{1,47} W. G. Li,¹ X. H. Li,^{55,43} X. L. Li,³⁷ X. N. Li,^{1,43} Z. B. Li,⁴⁴ Z. Y. Li,⁴⁴ H. Liang,^{1,47} H. Liang,^{55,43} Y. F. Liang,⁴⁰ Y. T. Liang,²⁸ G. R. Liao,¹² L. Z. Liao,^{1,47} J. Libby,²¹ C. X. Lin,⁴⁴ D. X. Lin,¹⁵ Y. J. Lin,¹³ B. Liu,^{38,h} B. J. Liu,¹ C. X. Liu,¹ D. Liu,^{55,43} D. Y. Liu,^{38,h} F. H. Liu,³⁹ Fang Liu,¹ Feng Liu,⁶ H. B. Liu,¹³ H. M. Liu,^{1,47} Huanhuan Liu,¹ Huihui Liu,¹⁷ J. B. Liu,^{55,43} J. Y. Liu,^{1,47} K. Liu,¹ K. Y. Liu,³¹ Ke Liu,⁶ L. Y. Liu,¹³ Q. Liu,⁴⁷ S. B. Liu,^{55,43} T. Liu,^{1,47} X. Liu,³⁰ X. Y. Liu,^{1,47} Y. B. Liu,³⁴ Z. A. Liu,^{1,43,47} Zhiqing Liu,³⁷ Y. F. Long,^{35,1} X. C. Lou,^{1,43,47} H. J. Lu,¹⁸ J. D. Lu,^{1,47} J. G. Lu,^{1,43} Y. Lu,¹ Y. P. Lu,^{1,43} C. L. Luo,³² M. X. Luo,⁶² P. W. Luo,⁴⁴ T. Luo,^{9,j} X. L. Luo,^{1,43} S. Lusso,^{58c} X. R. Lyu,⁴⁷ F. C. Ma,³¹ H. L. Ma,¹ L. L. Ma,³⁷ M. M. Ma,^{1,47} Q. M. Ma,¹ X. N. Ma,³⁴ X. X. Ma,^{1,47} X. Y. Ma,^{1,43} Y. M. Ma,³⁷ F. E. Maas,¹⁵ M. Maggiora,^{58a,58c} S. Maldaner,²⁶ S. Malde,⁵³ Q. A. Malik,⁵⁷ A. Mangoni,^{23b} Y. J. Mao,^{35,1} Z. P. Mao,¹ S. Marcello,^{58a,58c} Z. X. Meng,⁴⁹ J. G. Messchendorp,²⁹ G. Mezzadri,^{24a} J. Min,^{1,43} T. J. Min,³³ R. E. Mitchell,²² X. H. Mo,^{1,43,47} Y. J. Mo,⁶ C. Morales Morales,¹⁵ N. Yu. Muchnoi,^{10,d} H. Muramatsu,⁵¹ A. Mustafa,⁴ S. Nakhoul,^{11,g} Y. Nefedov,²⁷ F. Nerling,^{11,g} I. B. Nikolaev,^{10,d} Z. Ning,^{1,43} S. Nisar,^{8,k} S. L. Niu,^{1,43} S. L. Olsen,⁴⁷ Q. Ouyang,^{1,43,47} S. Pacetti,^{23b} Y. Pan,^{55,43} M. Papenbrock,⁵⁹ P. Patteri,^{23a} M. Pelizaeus,⁴ H. P. Peng,^{55,43} K. Peters,^{11,g} J. Pettersson,⁵⁹ J. L. Ping,³² R. G. Ping,^{1,47} A. Pitka,⁴ R. Poling,⁵¹ V. Prasad,^{55,43} H. R. Qi,² M. Qi,³³ T. Y. Qi,² S. Qian,^{1,43} C. F. Qiao,⁴⁷ N. Qin,⁶⁰ X. P. Qin,¹³ X. S. Qin,⁴ Z. H. Qin,^{1,43} J. F. Qiu,¹ S. Q. Qu,³⁴ K. H. Rashid,^{57,i} K. Ravindran,²¹ C. F. Redmer,²⁶ M. Richter,⁴ A. Rivetti,^{58c} V. Rodin,²⁹ M. Rolo,^{58c} G. Rong,^{1,47} Ch. Rosner,¹⁵ M. Rump,⁵² A. Sarantsev,^{27,e} M. Savrić,^{24b} Y. Schelhaas,²⁶ K. Schoenning,⁵⁹ W. Shan,¹⁹ X. Y. Shan,^{55,43} M. Shao,^{55,43} C. P. Shen,² P. X. Shen,³⁴ X. Y. Shen,^{1,47} H. Y. Sheng,¹ X. Shi,^{1,43} X. D. Shi,^{55,43} J. J. Song,³⁷ Q. Q. Song,^{55,43} X. Y. Song,¹ S. Sosio,^{58a,58c} C. Sowa,⁴ S. Spataro,^{58a,58c} F. F. Sui,³⁷ G. X. Sun,¹ J. F. Sun,¹⁶ L. Sun,⁶⁰ S. S. Sun,^{1,47} X. H. Sun,¹ Y. J. Sun,^{55,43} Y. K. Sun,^{55,43} Y. Z. Sun,¹ Z. J. Sun,^{1,43} Z. T. Sun,¹ Y. T. Tan,^{55,43} C. J. Tang,⁴⁰ G. Y. Tang,¹ X. Tang,¹ V. Thoren,⁵⁹ B. Tsednee,²⁵ I. Uman,^{46d} B. Wang,¹ B. L. Wang,⁴⁷ C. W. Wang,³³ D. Y. Wang,^{35,1} K. Wang,^{1,43} L. L. Wang,¹ L. S. Wang,¹ M. Wang,³⁷ M. Z. Wang,^{35,1} Meng Wang,^{1,47} P. L. Wang,¹ R. M. Wang,⁶¹ W. P. Wang,^{55,43} X. Wang,^{35,1} X. F. Wang,^{30,*} X. L. Wang,^{9,j} Y. Wang,⁴⁴ Y. Wang,^{55,43} Y. F. Wang,^{1,43,47} Y. Q. Wang,¹ Z. Wang,^{1,43} Z. G. Wang,^{1,43} Z. Y. Wang,¹ Zongyuan Wang,^{1,47} T. Weber,⁴ D. H. Wei,¹² P. Weidenkaff,²⁶ F. Weidner,⁵² H. W. Wen,³² S. P. Wen,¹ U. Wiedner,⁴ G. Wilkinson,⁵³ M. Wolke,⁵⁹ L. H. Wu,¹ L. J. Wu,^{1,47} Z. Wu,^{1,43} L. Xia,^{55,43} Y. Xia,²⁰ S. Y. Xiao,¹ Y. J. Xiao,^{1,47} Z. J. Xiao,³² Y. G. Xie,^{1,43} Y. H. Xie,⁶ T. Y. Xing,^{1,47} X. A. Xiong,^{1,47} Q. L. Xiu,^{1,43} G. F. Xu,¹ J. J. Xu,³³ L. Xu,¹ Q. J. Xu,¹⁴ W. Xu,^{1,47} X. P. Xu,⁴¹ F. Yan,⁵⁶ L. Yan,^{58a,58c} W. B. Yan,^{55,43} W. C. Yan,² Y. H. Yan,²⁰ H. J. Yang,^{38,h} H. X. Yang,¹ L. Yang,⁶⁰ R. X. Yang,^{55,43} S. L. Yang,^{1,47} Y. H. Yang,³³ Y. X. Yang,¹²

Yifan Yang,^{1,47} Z. Q. Yang,²⁰ M. Ye,^{1,43} M. H. Ye,⁷ J. H. Yin,¹ Z. Y. You,⁴⁴ B. X. Yu,^{1,43,47} C. X. Yu,³⁴ J. S. Yu,²⁰ T. Yu,⁵⁶
 C. Z. Yuan,^{1,47} X. Q. Yuan,^{35,1} Y. Yuan,¹ A. Yuncu,^{46b,a} A. A. Zafar,⁵⁷ Y. Zeng,²⁰ B. X. Zhang,¹ B. Y. Zhang,^{1,43}
 C. C. Zhang,¹ D. H. Zhang,¹ H. H. Zhang,⁴⁴ H. Y. Zhang,^{1,43} J. Zhang,^{1,47} J. L. Zhang,⁶¹ J. Q. Zhang,⁴ J. W. Zhang,^{1,43,47}
 J. Y. Zhang,¹ J. Z. Zhang,^{1,47} K. Zhang,^{1,47} L. Zhang,¹ S. F. Zhang,³³ T. J. Zhang,^{38,h} X. Y. Zhang,³⁷ Y. Zhang,^{55,43}
 Y. H. Zhang,^{1,43} Y. T. Zhang,^{55,43} Yang Zhang,¹ Yao Zhang,¹ Yi Zhang,^{9,j} Yu Zhang,⁴⁷ Z. H. Zhang,⁶ Z. P. Zhang,⁵⁵
 Z. Y. Zhang,⁶⁰ G. Zhao,¹ J. W. Zhao,^{1,43} J. Y. Zhao,^{1,47} J. Z. Zhao,^{1,43} Lei Zhao,^{55,43} Ling Zhao,¹ M. G. Zhao,³⁴ Q. Zhao,¹
 S. J. Zhao,⁶³ T. C. Zhao,¹ Y. B. Zhao,^{1,43} Z. G. Zhao,^{55,43} A. Zhemchugov,^{27,b} B. Zheng,⁵⁶ J. P. Zheng,^{1,43} Y. Zheng,^{35,1}
 Y. H. Zheng,⁴⁷ B. Zhong,³² L. Zhou,^{1,43} L. P. Zhou,^{1,47} Q. Zhou,^{1,47} X. Zhou,⁶⁰ X. K. Zhou,⁴⁷ X. R. Zhou,^{55,43}
 Xiaoyu Zhou,²⁰ Xu Zhou,²⁰ A. N. Zhu,^{1,47} J. Zhu,³⁴ J. Zhu,⁴⁴ K. Zhu,¹ K. J. Zhu,^{1,43,47} S. H. Zhu,⁵⁴ W. J. Zhu,³⁴ X. L. Zhu,⁴⁵
 Y. C. Zhu,^{55,43} Y. S. Zhu,^{1,47} Z. A. Zhu,^{1,47} J. Zhuang,^{1,43} B. S. Zou,¹ and J. H. Zou¹

(BESIII Collaboration)

¹*Institute of High Energy Physics, Beijing 100049, People's Republic of China*

²*Beihang University, Beijing 100191, People's Republic of China*

³*Beijing Institute of Petrochemical Technology, Beijing 102617, People's Republic of China*

⁴*Bochum Ruhr-University, D-44780 Bochum, Germany*

⁵*Carnegie Mellon University, Pittsburgh, Pennsylvania 15213, USA*

⁶*Central China Normal University, Wuhan 430079, People's Republic of China*

⁷*China Center of Advanced Science and Technology, Beijing 100190, People's Republic of China*

⁸*COMSATS University Islamabad, Lahore Campus, Defence Road, Off Raiwind Road, 54000 Lahore, Pakistan*

⁹*Fudan University, Shanghai 200443, People's Republic of China*

¹⁰*G.I. Budker Institute of Nuclear Physics SB RAS (BINP), Novosibirsk 630090, Russia*

¹¹*GSI Helmholtzcentre for Heavy Ion Research GmbH, D-64291 Darmstadt, Germany*

¹²*Guangxi Normal University, Guilin 541004, People's Republic of China*

¹³*Guangxi University, Nanning 530004, People's Republic of China*

¹⁴*Hangzhou Normal University, Hangzhou 310036, People's Republic of China*

¹⁵*Helmholtz Institute Mainz, Johann-Joachim-Becher-Weg 45, D-55099 Mainz, Germany*

¹⁶*Henan Normal University, Xinxiang 453007, People's Republic of China*

¹⁷*Henan University of Science and Technology, Luoyang 471003, People's Republic of China*

¹⁸*Huangshan College, Huangshan 245000, People's Republic of China*

¹⁹*Hunan Normal University, Changsha 410081, People's Republic of China*

²⁰*Hunan University, Changsha 410082, People's Republic of China*

²¹*Indian Institute of Technology Madras, Chennai 600036, India*

²²*Indiana University, Bloomington, Indiana 47405, USA*

^{23a}*INFN Laboratori Nazionali di Frascati, I-00044, Frascati, Italy*

^{23b}*INFN and University of Perugia, I-06100, Perugia, Italy*

^{24a}*INFN Sezione di Ferrara, I-44122, Ferrara, Italy*

^{24b}*University of Ferrara, I-44122, Ferrara, Italy*

²⁵*Institute of Physics and Technology, Peace Ave. 54B, Ulaanbaatar 13330, Mongolia*

²⁶*Johannes Gutenberg University of Mainz, Johann-Joachim-Becher-Weg 45, D-55099 Mainz, Germany*

²⁷*Joint Institute for Nuclear Research, 141980 Dubna, Moscow region, Russia*

²⁸*Justus-Liebig-Universität Giessen, II. Physikalisches Institut, Heinrich-Buff-Ring 16, D-35392 Giessen, Germany*

²⁹*KVI-CART, University of Groningen, NL-9747 AA Groningen, Netherlands*

³⁰*Lanzhou University, Lanzhou 730000, People's Republic of China*

³¹*Liaoning University, Shenyang 110036, People's Republic of China*

³²*Nanjing Normal University, Nanjing 210023, People's Republic of China*

³³*Nanjing University, Nanjing 210093, People's Republic of China*

³⁴*Nankai University, Tianjin 300071, People's Republic of China*

³⁵*Peking University, Beijing 100871, People's Republic of China*

³⁶*Shandong Normal University, Jinan 250014, People's Republic of China*

³⁷*Shandong University, Jinan 250100, People's Republic of China*

³⁸*Shanghai Jiao Tong University, Shanghai 200240, People's Republic of China*

³⁹*Shanxi University, Taiyuan 030006, People's Republic of China*

⁴⁰*Sichuan University, Chengdu 610064, People's Republic of China*

⁴¹*Soochow University, Suzhou 215006, People's Republic of China*

⁴²*Southeast University, Nanjing 211100, People's Republic of China*

⁴³*State Key Laboratory of Particle Detection and Electronics, Beijing 100049, Hefei 230026, People's Republic of China*

- ⁴⁴*Sun Yat-Sen University, Guangzhou 510275, People's Republic of China*
⁴⁵*Tsinghua University, Beijing 100084, People's Republic of China*
^{46a}*Ankara University, 06100 Tandogan, Ankara, Turkey*
^{46b}*Istanbul Bilgi University, 34060 Eyup, Istanbul, Turkey*
^{46c}*Uludag University, 16059 Bursa, Turkey*
^{46d}*Near East University, Nicosia, North Cyprus, Mersin 10, Turkey*
⁴⁷*University of Chinese Academy of Sciences, Beijing 100049, People's Republic of China*
⁴⁸*University of Hawaii, Honolulu, Hawaii 96822, USA*
⁴⁹*University of Jinan, Jinan 250022, People's Republic of China*
⁵⁰*University of Manchester, Oxford Road, Manchester, M13 9PL, United Kingdom*
⁵¹*University of Minnesota, Minneapolis, Minnesota 55455, USA*
⁵²*University of Muenster, Wilhelm-Klemm-Str. 9, 48149 Muenster, Germany*
⁵³*University of Oxford, Keble Rd, Oxford, United Kingdom OX13RH*
⁵⁴*University of Science and Technology Liaoning, Anshan 114051, People's Republic of China*
⁵⁵*University of Science and Technology of China, Hefei 230026, People's Republic of China*
⁵⁶*University of South China, Hengyang 421001, People's Republic of China*
⁵⁷*University of the Punjab, Lahore-54590, Pakistan*
^{58a}*University of Turin, I-10125, Turin, Italy*
^{58b}*University of Eastern Piedmont, I-15121, Alessandria, Italy*
^{58c}*INFN, I-10125, Turin, Italy*
⁵⁹*Uppsala University, Box 516, SE-75120 Uppsala, Sweden*
⁶⁰*Wuhan University, Wuhan 430072, People's Republic of China*
⁶¹*Xinyang Normal University, Xinyang 464000, People's Republic of China*
⁶²*Zhejiang University, Hangzhou 310027, People's Republic of China*
⁶³*Zhengzhou University, Zhengzhou 450001, People's Republic of China*



(Received 14 October 2019; revised manuscript received 5 December 2019; published 24 January 2020)

Using a total of 11.0 fb^{-1} of e^+e^- collision data with center-of-mass energies between 4.009 and 4.6 GeV and collected with the BESIII detector at BEPCII, we measure fifteen exclusive cross sections and effective form factors for the process $e^+e^- \rightarrow \Xi^-\bar{\Xi}^+$ by means of a single baryon-tag method. After performing a fit to the dressed cross section of $e^+e^- \rightarrow \Xi^-\bar{\Xi}^+$, no significant $\psi(4230)$ or $\psi(4260)$ resonance is observed in the $\Xi^-\bar{\Xi}^+$ final states, and upper limits at the 90% confidence level on $\Gamma_{ee}\mathcal{B}$ for the processes $\psi(4230)/\psi(4260) \rightarrow \Xi^-\bar{\Xi}^+$ are determined. In addition, an excited Ξ baryon at $1820 \text{ MeV}/c^2$ is observed with a statistical significance of $6.2\text{--}6.5\sigma$ by including the systematic uncertainty, and the mass and width are measured to be $M = (1825.5 \pm 4.7 \pm 4.7) \text{ MeV}/c^2$ and $\Gamma = (17.0 \pm 15.0 \pm 7.9) \text{ MeV}$, which confirms the existence of the $J^P = \frac{3}{2}^-$ state $\Xi(1820)$.

DOI: [10.1103/PhysRevLett.124.032002](https://doi.org/10.1103/PhysRevLett.124.032002)

In the last decade, a series of charmonium-like states have been observed at e^+e^- colliders. The study of the production of charmonium-like states with the quantum number $J^{PC} = 1^{--}$ above the open charm threshold in e^+e^- annihilations and their subsequent two-body hadronic decays provides a test for QCD calculations [1,2]. According to potential models, there are five vector charmonium states between the $1D$ state [$\psi(3773)$] and $4.7 \text{ GeV}/c^2$, namely, the $3S$, $2D$, $4S$, $3D$, and $5S$ states [1]. From experimental studies, besides the three well-established structures observed in the inclusive

hadronic cross section [3], i.e., $\psi(4040)$, $\psi(4160)$, and $\psi(4415)$, five new states, i.e., $\psi(4230)$, $\psi(4260)$, $\psi(4360)$, $\psi(4634)$, and $\psi(4660)$ have been reported in initial state radiation (ISR) processes, i.e., $e^+e^- \rightarrow \gamma_{\text{ISR}}\pi^+\pi^-J/\psi$ or $e^+e^- \rightarrow \gamma_{\text{ISR}}\pi^+\pi^-\psi(3686)$ at the BABAR [4] and Belle [5], or in direct production processes at the CLEO [6] and BESIII experiments [7]. Surprisingly, up to now, no evidence for baryon antibaryon pairs above open charm production associated with these states has been found except for the $\psi(4634)$ resonance observed in $\Lambda_c^+\bar{\Lambda}_c^-$ [8]. Although the BESIII Collaboration previously performed a search for baryonic decays of $\psi(4040)$ [9], including $\Xi^-\bar{\Xi}^+$ final states based on a full reconstruction method, no candidates were observed. The overpopulation of structures in this mass region and the mismatch of the properties between the potential model predictions and experimental measurements make them good candidates for exotic states. Various

Published by the American Physical Society under the terms of the Creative Commons Attribution 4.0 International license. Further distribution of this work must maintain attribution to the author(s) and the published article's title, journal citation, and DOI. Funded by SCOAP³.

scenarios, which interpret one or some of them as hybrid states, tetraquark states, or molecular states [10], have been proposed.

The electromagnetic structure of hadrons, parametrized in terms of electromagnetic form factors (EMFFs) [11], provides a key to understanding QCD effects in bound states. While the nucleon has been studied rigorously for more than sixty years, new techniques and the availability of data with larger statistics from modern facilities have given rise to a renewed interest in the field, i.e., the proton radius puzzle [16]. The access to hyperon structure by EMFFs provides an extra dimension that inspires measurements of exclusive cross sections and EMFFs for baryon antibaryon pairs above open charm threshold.

The constituent quark model has been very successful in describing the ground state of the flavor SU(3) octet and decuplet baryons [3,17]. However, some observed excited states do not agree well with the theoretical prediction. It is thus important to study such unusual states, both to probe the limitation of the quark models and to spot unrevealed aspects of the QCD description of the structure of hadron resonances. Intriguingly, the Ξ resonances with strangeness $S = -2$ may provide important information on the latter aspect. Although there has been significant progress in the experimental studies of charmed baryons by the BABAR [18], LHCb [19], and Belle [20,21] Collaborations, doubly charm baryons by the LHCb Collaboration [22], doubly strange baryons by the Belle Collaboration [23], the studies of excited Ξ states are still sparse [3]. Neither the first radial excitation with spin parity of $J^P = \frac{1}{2}^+$ nor a first orbital excitation with $J^P = \frac{1}{2}^-$ have been identified. Determination of the resonance parameters of the first excited state is a vital test of our understanding of the structure of Ξ resonances, where one of candidates for the first excited state is $\Xi(1690)$ with a three-star rating on a four-star scale [3], the second one is $\Xi(1620)$ with one-star rating, and another excited state is $\Xi(1820)$ with a three-star rating [3], for which the spin was previously determined to be $J = \frac{3}{2}$ [24], and subsequently the parity was determined to be negative and the spin parity confirmed to be $J^P = \frac{3}{2}^-$ by another experiment [25].

In this Letter, we present a measurement of the Born cross section and the effective form factors (EFF) [11] for the process $e^+e^- \rightarrow \Xi^-\bar{\Xi}^+$, an estimation of the upper limit on $\Gamma_{ee}\mathcal{B}[\psi(4230)/\psi(4260) \rightarrow \Xi^-\bar{\Xi}^+]$ at the 90% confidence level (C.L.), and the observation of an excited Ξ baryon at 1820 MeV/ c^2 . The dataset used in this analysis corresponds to a total of 11.0 fb $^{-1}$ of e^+e^- collision data [11] collected at center-of-mass (c.m.) energies from 4.009 to 4.6 GeV with the BESIII detector [26] at BEPCII [27].

The selection of $e^+e^- \rightarrow \Xi^-\bar{\Xi}^+$ events with a full reconstruction method has low-reconstruction efficiency. Here, to achieve higher efficiency, a single baryon Ξ^- tag technique is employed, i.e., only one Ξ^- baryon is

reconstructed by the $\pi^-\Lambda$ decay mode with $\Lambda \rightarrow p\pi^-$, and the antibaryon $\bar{\Xi}^+$ is extracted from the recoil side (unless otherwise noted, the charge-conjugate state of the Ξ^- mode is included by default below). To determine the detection efficiency for the decay $e^+e^- \rightarrow \Xi^-\bar{\Xi}^+$, 100 k simulated events are generated for each of 15 energy points in the range of 4.009 to 4.6 GeV according to phase space using the KKMC generator [28], which includes the ISR effect. The Ξ^- is simulated in its decay to the $\pi^-\Lambda$ mode with the subsequent decay $\Lambda \rightarrow p\pi^-$ via EvtGen [29], and the antibaryons are allowed to decay inclusively. The response of the BESIII detector is modeled with Monte Carlo (MC) simulations using a framework based on GEANT4 [30]. Large simulated samples of generic $e^+e^- \rightarrow$ hadrons events (“inclusive MC”) are used to estimate background conditions.

Charged tracks are required to be reconstructed in the main drift chamber (MDC) with good helical fits and within the angular coverage of the MDC: $|\cos\theta| < 0.93$, where θ is the polar angle with respect to the e^+ beam direction. Information from the specific energy deposition (dE/dx) measured in the MDC combined with the time of flight (TOF) is used to form particle identification (PID) confidence levels for the hypotheses of a pion, kaon, and proton. Each track is assigned to the particle type with the highest C.L. Events with at least two negatively charged pions and one proton are kept for further analysis.

To reconstruct Λ candidates, a secondary vertex fit is applied to all $p\pi^-$ combinations; the ones characterized by $\chi^2 < 500$ with 3 degrees of freedom are kept for further analysis. The $p\pi^-$ invariant mass is required to be within 5 MeV/ c^2 of the nominal Λ mass, determined by optimizing the figure of merit $S/\sqrt{S+B}$ based on the MC simulation, where S is the number of signal MC events and B is the number of the background events expected from simulation. To further suppress background from non- Λ events, the Λ decay length is required to be greater than zero, where negative decay lengths are caused by the limited detector resolution.

The Ξ^- candidates are reconstructed with a similar strategy using a secondary vertex fit, and the candidate with the minimum value of $|M_{\pi^-\Lambda} - m_{\Xi^-}|$ from all $\pi^-\Lambda$ combinations is selected, where $M_{\pi^-\Lambda}$ is the invariant mass of the $\pi^-\Lambda$ pair, and m_{Ξ^-} is the nominal mass of Ξ^- from the PDG [3]. Further $M_{\pi^-\Lambda}$ is required to be within 10 MeV/ c^2 of the nominal Ξ^- mass, and the Ξ^- decay length L_{Ξ^-} (cm) is required to be greater than zero.

To obtain the antibaryon candidates $\bar{\Xi}^+$, we use the distribution of mass recoiling against the selected $\pi^-\Lambda$ system,

$$M_{\pi^-\Lambda}^{\text{recoil}} = \sqrt{(\sqrt{s} - E_{\pi^-\Lambda})^2 - |\vec{p}_{\pi^-\Lambda}|^2}, \quad (1)$$

where $E_{\pi^-\Lambda}$ and $\vec{p}_{\pi^-\Lambda}$ are the energy and momentum of the selected $\pi^-\Lambda$ candidate in the c.m. system, and \sqrt{s} is the

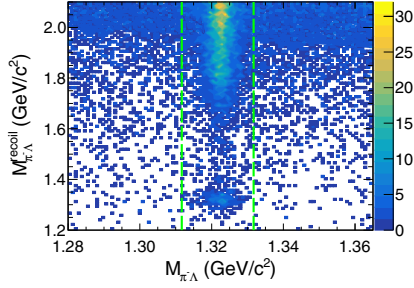


FIG. 1. Distribution of $M_{\pi^- \Lambda}$ versus $M_{\pi^- \Lambda}^{\text{recoil}}$ for sum of 15 energy points. The dashed lines denote the Ξ^- signal region.

c.m. energy. Figure 1 shows the distribution of $M_{\pi^- \Lambda}$ versus $M_{\pi^- \Lambda}^{\text{recoil}}$ for all 15 considered energy points.

The signal yields for the decay $e^+e^- \rightarrow \Xi^- \bar{\Xi}^+$ at each energy point are determined by performing an extended maximum likelihood fit to the $M_{\pi^- \Lambda}^{\text{recoil}}$ spectrum in the range from 1.2 to 1.5 GeV/c^2 . In the fit, the signal shape for the decay $e^+e^- \rightarrow \Xi^- \bar{\Xi}^+$ at each energy point is represented by the simulated MC shape. After applying the same event selection as the data on the inclusive MC samples at each c.m. energy, it is found that few background events remain at each energy point coming from $e^+e^- \rightarrow \pi^+ \pi^- J/\psi$, $J/\psi \rightarrow \Lambda \bar{\Lambda}$ events, and they are distributed smoothly in the region of interest and can be described by a second-order polynomial function. Figure 2 shows the $M_{\pi^- \Lambda}^{\text{recoil}}$ distributions for the decay $e^+e^- \rightarrow \Xi^- \bar{\Xi}^+$ at each energy point.

The Born cross section for $e^+e^- \rightarrow \Xi^- \bar{\Xi}^+$ is calculated by

$$\sigma^B(s) = \frac{N_{\text{obs}}}{2\mathcal{L}(1+\delta) \frac{1}{|1-\Pi|^2} \epsilon \mathcal{B}(\Xi^- \rightarrow \pi^- \Lambda) \mathcal{B}(\Lambda \rightarrow p \pi^-)}, \quad (2)$$

where N_{obs} is the number of the observed signal events, \mathcal{L} is the integrated luminosity related to the c.m. energy, $(1+\delta)$ is the ISR correction factor [31], $1/(|1-\Pi|^2)$ is the vacuum polarization correction factor [32], ϵ is the detection efficiency, and $\mathcal{B}(\Xi^- \rightarrow \pi^- \Lambda)$ and $\mathcal{B}(\Lambda \rightarrow p \pi^-)$ are the branching fractions taken from the PDG [3]. The ISR correction factor is obtained using the QED calculation as described in Ref. [33] and taking the formula used to fit the cross section measured in this analysis parametrized after two iterations as input. The measured cross sections and EFFs are shown in Fig. 3 and summarized in the Supplemental Material [11]. The Supplemental Material also contains the details of the cross section and EFF calculations.

A maximum likelihood method is used to fit the dressed cross section $\sigma^{\text{dressed}} = \sigma^B/|1-\Pi|^2$, for the process $e^+e^- \rightarrow \Xi^- \bar{\Xi}^+$ parametrized as the coherent sum of a power-law function plus a Breit-Wigner (BW) function for $\psi(4230)$ or $\psi(4260)$,

$$\sigma^{\text{dressed}}(\sqrt{s}) = \left| c_0 \frac{\sqrt{P(\sqrt{s})}}{s^n} + e^{i\phi} \text{BW}(\sqrt{s}) \sqrt{\frac{P(\sqrt{s})}{P(M)}} \right|^2, \quad (3)$$

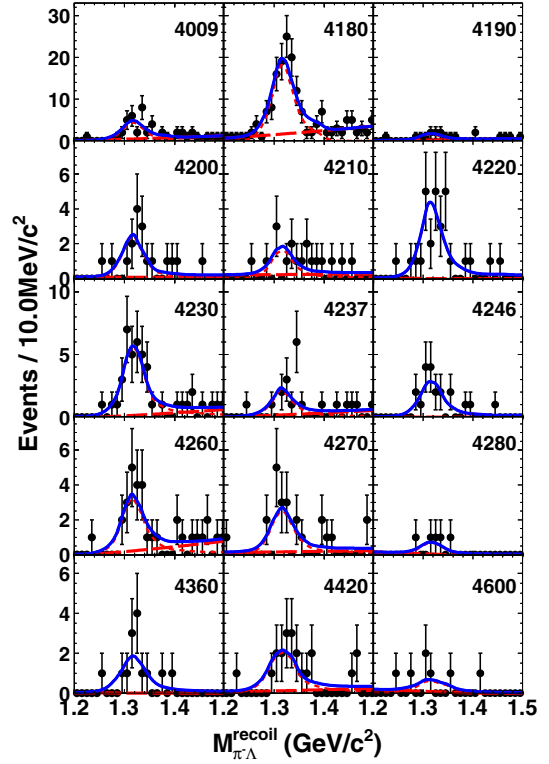


FIG. 2. Fit to the recoil mass spectra of $\pi^- \Lambda$ at each energy point in units of MeV/c^2 . Dots with error bars are data, the blue solid lines show the fit result, the red short-dashed lines are for signal, and the red long-dashed ones are for the smooth background.

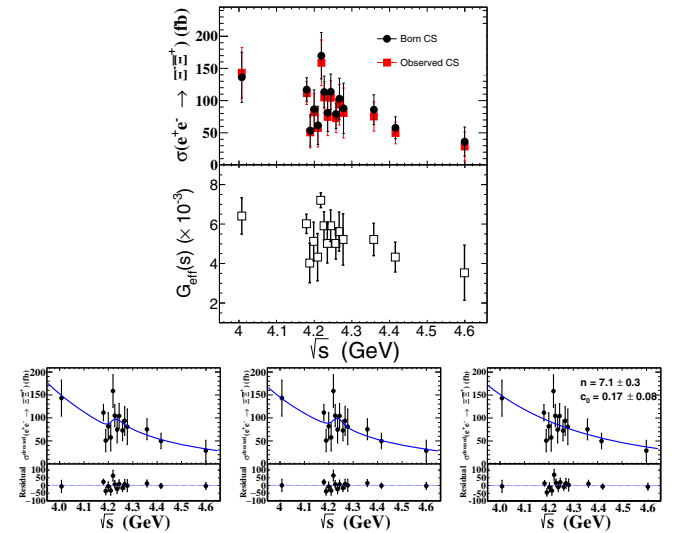


FIG. 3. Top: cross section (points with error bars) and EFF (open boxes with error bars). Bottom: fits to the dressed cross sections at c.m. energies from 4.009 to 4.6 GeV with the assumptions of a power-law function plus a $\psi(4230)$ resonance function (left) or a $\psi(4260)$ resonance function (middle), and without resonance assumption (right) where the dots with error bars are the dressed cross sections and the solid lines show the fit results.

where the mass M and total width Γ are fixed to the $\psi(4230)/\psi(4260)$ resonance with PDG values [3], ϕ is the relative phase between the BW function,

$$\text{BW}(\sqrt{s}) = \frac{\sqrt{12\pi\Gamma_{ee}\mathcal{B}\Gamma}}{s - M^2 + iM\Gamma}, \quad (4)$$

and power function, n is a free fit parameter, and $P(\sqrt{s})$ is the two-body phase space factor. The $\psi(4230)$ and $\psi(4260) \rightarrow \Xi^-\bar{\Xi}^+$ processes are found to be not significant. Therefore, upper limits on the products of the two-electron partial width and the branching fractions of $\psi(4230)$ and $\psi(4260) \rightarrow \Xi^-\bar{\Xi}^+$ ($\Gamma_{ee}\mathcal{B}$) at the 90% credible level are estimated using a Bayesian approach [34] to be $\Gamma_{ee}\mathcal{B}_{\psi(4230)} < 0.33 \times 10^{-3}$ eV and $\Gamma_{ee}\mathcal{B}_{\psi(4260)} < 0.27 \times 10^{-3}$ eV taking into account the systematic uncertainty described later. Here the masses and widths of $\psi(4230)$ and $\psi(4260)$ are changed by all combinations of $\pm 1\sigma$, and the estimation of the upper limits repeated. The largest ones are taken as the final results. Figure 3 shows the fit to the dressed cross section assuming the $\psi(4230)$ or the $\psi(4260)$ resonance and without resonance assumption. Including systematic uncertainties, the significance for both resonances is calculated to be $\sim 2.7\sigma$.

The EFF for $e^+e^- \rightarrow \Xi^-\bar{\Xi}^+$ is calculated by the formula [11]

$$|G_{\text{eff}}(s)| = \sqrt{\frac{3s\sigma^B}{4\pi\alpha^2 C\beta \left(1 + \frac{2m_{\Xi^-}^2}{s}\right)}}, \quad (5)$$

where α is the fine structure constant, m_{Ξ^-} is the mass of Ξ^- , the variable $\beta = \sqrt{1 - (1/\tau)}$ is the velocity, $\tau = s/4m_{\Xi^-}^2$, and the Coulomb correction factor C [14] parametrizes the electromagnetic interaction between the outgoing baryon and antibaryon. For neutral baryons, the Coulomb factor is unity, while for pointlike charged fermions $C = (\pi\alpha/\beta) \cdot (\sqrt{1 - \beta^2}/1 - e^{-\pi\alpha/\beta})$ [35–37]. Figure 3 shows the measured EFFs of $e^+e^- \rightarrow \Xi^-\bar{\Xi}^+$.

Based on the selected data for the sum of 15 energy points, an excited Ξ baryon is observed in the $M_{\pi^-\Lambda}^{\text{recoil}}$ range from 1.6 to 2.1 GeV/ c^2 . Figure 4 shows a fit to the recoil mass spectrum of $\pi^-\Lambda$, where the signal is described by a BW function convolved with a double Gaussian function, and the background is described by a 2nd order Chebyshev polynomial, where the resolution width of Gaussian function is fixed according to the MC simulation. The number of signal events is 288_{-85}^{+125} , and the mass and width are measured to be $M = (1825.5 \pm 4.7)$ MeV/ c^2 and $\Gamma = (17.0 \pm 15.0)$ MeV, where the uncertainties are statistical only. The statistical significance of the 1820 MeV/ c^2 resonance is estimated to be 6.2–6.5 σ with including the systematic uncertainty.

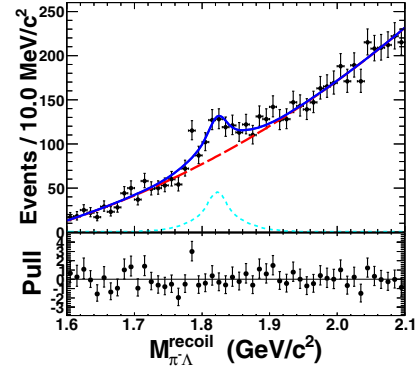


FIG. 4. Fit to the recoil mass of $\pi\Lambda$ of the combined data of the 15 energy points in the range from 1.6 to 2.1 GeV/ c^2 . Dots with error bars are data, the blue solid line shows the fit result, the short-dashed line is for the signal, and the long-dashed one is for the background.

Systematic uncertainties on the measurements of the cross section originate from the luminosity measurement, branching fractions of $\Xi^- \rightarrow \pi^-\Lambda$ and $\Lambda \rightarrow p\pi^-$, detection efficiency, ISR correction factor, line-shape structure, angular distribution, and the fit procedure. The uncertainty due to the vacuum polarization is negligible. The integrated luminosity is measured with a precision of 1.0% [12]. The branching fraction uncertainties for $\Xi^- \rightarrow \pi^-\Lambda$ and $\Lambda \rightarrow p\pi^-$ are 0.1% and 0.8% from the PDG [3]. The systematic sources of the uncertainty for the detection efficiency include the Ξ^- reconstruction, the mass windows of Ξ^-/Λ , and the decay lengths of Ξ^-/Λ . The Ξ^- reconstruction is studied using the same method as described in Ref. [38], and an uncertainty of 6.6% is found. The mass windows of Ξ^- and Λ are studied by varying the nominal requirements by 5.0 MeV/ c^2 , which yield uncertainties of 0.7% and 3.2%, respectively. The decay lengths of Λ and Ξ^- are studied with and without the nominal requirements, and the uncertainties are estimated to be 1.5% and 1.7%, respectively. For the ISR correction factor, we iterate the cross section measurement until $(1 + \delta)\epsilon$ converges as described in Ref. [39]. The change due to the different criteria for convergence is taken as the systematic uncertainty. The uncertainty due to the line-shape structure is estimated to be 4.8% with the assumption of $\psi(4230)/\psi(4260) \rightarrow \Xi^-\bar{\Xi}^+$. The uncertainty due to the angular distribution is estimated to be 4.0% by weighting the $\cos\theta_{\Xi}$ difference for each bin between the data and the phase space MC model, where the θ_{Ξ} is the angle between Ξ and the beam directions in the e^+e^- c.m. system [38]. The systematic sources of the uncertainty in the fit of the $M_{\pi^-\Lambda}^{\text{recoil}}$ spectrum include the fitting range, the polynomial shape, the mass resolution, the signal shape the mass windows of Ξ^-/Λ , and the decay lengths of Ξ^-/Λ . The uncertainty due to the fit range is estimated to be 3.3% by varying the mass range by ± 50 MeV/ c^2 . The uncertainty due to the polynomial function is estimated to be 3.3% by

alternative fits with a third- or a first-order polynomial function. The mass resolution is studied by varying the nominal signal shape convolved with a Gaussian function, and the yield difference is taken as a systematic uncertainty, which is 4.0%. The effect due to the signal shape is studied by varying the resolution in the convolution of the Breit-Wigner with a Gaussian function. This gives an uncertainty of 3.2%. The effect of the MC statistics on the used signal shape is studied by using a MC sample with only 10% of the events compared to the nominal fit, and the uncertainty is 0.5%. Assuming all sources to be independent, the total systematic uncertainty on the cross section measurement for $e^+e^- \rightarrow \Xi^-\bar{\Xi}^+$ is determined to be 12.7% by the quadratic sum of these sources.

Systematic uncertainties on the measurements of the mass and width for the excited Ξ state mainly originate from the fit range, the background shape, the mass resolution, and the signal shape. The fit range, the background, and signal shapes are studied with the same method as above with mass uncertainties of 1.5, 1.3, and 1.9 MeV/ c^2 , and width uncertainties of 5.6, 3.4, and 4.5 MeV, respectively. The mass uncertainty due to the mass resolution is determined to be 3.8 MeV/ c^2 by calibrating the resolution difference in the Ξ^- mass region with the full data sample. The total systematic uncertainties of mass and width are calculated to be 4.7 MeV/ c^2 and 7.9 MeV, respectively, by summing independent systematic sources in quadrature.

In summary, using a total of 11.0 fb $^{-1}$ of e^+e^- collision data above the open-charm threshold collected with the BESIII detector at the BEPCII collider, we have studied the process $e^+e^- \rightarrow \Xi^-\bar{\Xi}^+$ based on a single baryon tag technique. We have measured fifteen exclusive Born cross sections and EFFs in the range from 4.009 to 4.6 GeV/ c^2 , where the form factors for the process $e^+e^- \rightarrow \Xi^-\bar{\Xi}^+$ have not been previously measured due to limited statistics. A fit to the dressed cross section for $e^+e^- \rightarrow \Xi^-\bar{\Xi}^+$ with the assumptions of a power-law dependence for continuum plus a $\psi(4230)$ or $\psi(4260)$ resonance is performed, and no significant signal for the processes $\psi(4230)$ or $\psi(4260) \rightarrow \Xi^-\bar{\Xi}^+$ is observed. The upper limits on the products of the electronic partial width and the branching fractions of $\psi(4230)$ and $\psi(4260) \rightarrow \Xi^-\bar{\Xi}^+$ are measured to be $\Gamma_{ee}\mathcal{B}_{\psi(4230)} < 0.33 \times 10^{-3}$ eV and $\Gamma_{ee}\mathcal{B}_{\psi(4260)} < 0.27 \times 10^{-3}$ eV at 90% C.L., which may help to understand the nature of $\psi(4260)$ [40,41]. In particular, charmless decays of the $\psi(4260)$ are expected by the hybrid model [41]. In addition, an excited Ξ baryon at ~ 1820 MeV/ c^2 is observed with a statistical significance of 6.2–6.5 σ by including the systematic uncertainty, and the mass and width are measured to be $M = (1825.5 \pm 4.7 \pm 4.7)$ MeV/ c^2 and $\Gamma = (17.0 \pm 15.0 \pm 7.9)$ MeV, which are consistent with the mass and width of $\Xi(1820)^-$ obtained from the PDG [3] within 1 σ uncertainty. The results shed light on the structure of hyperon resonances with strangeness $S = -2$.

The BESIII Collaboration thanks the staff of BEPCII and the IHEP computing center for their strong support. This work is supported in part by National Key Basic Research Program of China under Contract No. 2015CB856700; China Postdoctoral Science Foundation under Contract No. 2018M630206; National Natural Science Foundation of China (NSFC) under Contracts No. 11521505, No. 11625523, No. 11635010, No. 11675184, No. 11705209, No. 11735014, No. 11822506, No. 11835012, No. 11875115, No. 11905236; Chinese Academy of Science Focused Science Grant; National 1000 Talents Program of China; the Chinese Academy of Sciences (CAS) Large-Scale Scientific Facility Program; Joint Large-Scale Scientific Facility Funds of the NSFC and CAS under Contracts No. U1532257, No. U1532258, No. U1732263, No. U1832207; CAS Key Research Program of Frontier Sciences under Contracts No. QYZDJ-SSW-SLH003, No. QYZDJ-SSW-SLH040; 100 Talents Program of CAS; Institute of Nuclear and Particle Physics, Astronomy and Cosmology (INPAC) and Shanghai Key Laboratory for Particle Physics and Cosmology; ERC under Contract No. 758462; German Research Foundation DFG under Contracts Nos. Collaborative Research Center CRC 1044, FOR 2359; Istituto Nazionale di Fisica Nucleare, Italy; Koninklijke Nederlandse Akademie van Wetenschappen (KNAW) under Contract No. 530-4CDP03; Ministry of Development of Turkey under Contract No. DPT2006K-120470; National Science and Technology fund; STFC (United Kingdom); The Knut and Alice Wallenberg Foundation (Sweden) under Contract No. 2016.0157; The Royal Society, UK under Contracts No. DH140054, No. DH160214; The Swedish Research Council; U.S. Department of Energy under Contracts No. DE-FG02-05ER41374, No. DE-SC-0010118, No. DE-SC-0012069; University of Groningen (RuG) and the Helmholtzzentrum fuer Schwerionenforschung GmbH (GSI), Darmstadt.

^aAlso at Bogazici University, 34342 Istanbul, Turkey.

^bAlso at the Moscow Institute of Physics and Technology, Moscow 141700, Russia.

^cAlso at the Functional Electronics Laboratory, Tomsk State University, Tomsk, 634050, Russia.

^dAlso at the Novosibirsk State University, Novosibirsk, 630090, Russia.

^eAlso at the NRC ‘‘Kurchatov Institute,’’ PNPI, 188300, Gatchina, Russia.

^fAlso at Istanbul Arel University, 34295 Istanbul, Turkey.

^gAlso at Goethe University Frankfurt, 60323 Frankfurt am Main, Germany.

^hAlso at Key Laboratory for Particle Physics, Astrophysics and Cosmology, Ministry of Education; Shanghai Key Laboratory for Particle Physics and Cosmology; Institute of Nuclear and Particle Physics, Shanghai 200240, People’s Republic of China.

ⁱAlso at Government College Women University, Sialkot—51310. Punjab, Pakistan.

- ^jAlso at Key Laboratory of Nuclear Physics and Ion-beam Application (MOE) and Institute of Modern Physics, Fudan University, Shanghai 200443, People's Republic of China.
- ^kAlso at Harvard University, Department of Physics, Cambridge, Massachusetts, 02138, USA.
- ^lAlso at State Key Laboratory of Nuclear Physics and Technology, Peking University, Beijing 100871, People's Republic of China.
- *Corresponding author.
wangxiongfei@lzu.edu.cn
- [1] N. Brambilla *et al.*, *Eur. Phys. J. C* **71**, 1534 (2011).
- [2] R. A. Briceno *et al.*, *Chin. Phys. C* **40**, 042001 (2016).
- [3] M. Tanabashi *et al.* (Particle Data Group), *Phys. Rev. D* **98**, 030001 (2018); G. Pakhlova and V. Zhukova, *Proc. Sci., Hadron2017* (2018) 011.
- [4] B. Aubert *et al.* (BABAR Collaboration), *Phys. Rev. Lett.* **95**, 142001 (2005); **98**, 212001 (2007); J. P. Lees *et al.* (BABAR Collaboration), *Phys. Rev. D* **89**, 111103 (2014); **86**, 051102(R) (2012).
- [5] C. Z. Yuan *et al.* (Belle Collaboration), *Phys. Rev. Lett.* **99**, 182004 (2007); X. L. Wang *et al.* (Belle Collaboration), *Phys. Rev. Lett.* **99**, 142002 (2007); *Phys. Rev. D* **91**, 112007 (2015); G. Pakhlova *et al.* (Belle Collaboration), *Phys. Rev. Lett.* **101**, 172001 (2008); Z. Q. Liu *et al.* (Belle Collaboration), *Phys. Rev. Lett.* **110**, 252002 (2013).
- [6] T. E. Coan *et al.* (CLEO Collaboration), *Phys. Rev. Lett.* **96**, 162003 (2006).
- [7] M. Ablikim *et al.* (BESIII Collaboration), *Phys. Rev. Lett.* **114**, 092003 (2015).
- [8] G. Pakhlova *et al.* (Belle Collaboration), *Phys. Rev. Lett.* **101**, 172001 (2008).
- [9] M. Ablikim *et al.* (BESIII Collaboration), *Phys. Rev. D* **87**, 112011 (2013).
- [10] H. X. Chen, W. Chen, X. Liu, and S. L. Zhu, *Phys. Rep.* **639**, 1 (2016).
- [11] See Supplemental Material at <http://link.aps.org/supplemental/10.1103/PhysRevLett.124.032002> for a summary of number of signal events, luminosity, detection efficiency, ISR factor, vacuum polarization factor, the Born cross section, the effective form factor, statistical significance at each energy point, which includes Refs. [12–15].
- [12] M. Ablikim *et al.* (BESIII Collaboration), *Chin. Phys. C* **39**, 093001 (2015).
- [13] M. Ablikim *et al.* (BESIII Collaboration), *Chin. Phys. C* **40**, 063001 (2016).
- [14] R. Baldini, S. Pacetti, A. Zallo, and A. Zichichi, *Eur. Phys. J. A* **39**, 315 (2009).
- [15] B. Aubert *et al.* (BABAR Collaboration), *Phys. Rev. D* **73**, 012005 (2006).
- [16] R. Pohl *et al.*, *Nature (London)* **466**, 213 (2010).
- [17] K. T. Chao, N. Isgur, and G. Karl, *Phys. Rev. D* **23**, 155 (1981); S. Godfrey and N. Isgur, *Phys. Rev. D* **32**, 189 (1985); S. Capstick and N. Isgur, *Phys. Rev. D* **34**, 2809 (1986).
- [18] B. Aubert *et al.* (BABAR Collaboration), *Phys. Rev. Lett.* **98**, 012001 (2007).
- [19] R. Aaij *et al.* (LHCb Collaboration), *Phys. Rev. Lett.* **118**, 182001 (2017).
- [20] J. Yelton *et al.* (Belle Collaboration), *Phys. Rev. D* **97**, 051102 (2018).
- [21] Y. B. Li *et al.* (Belle Collaboration), *Eur. Phys. J. C* **78**, 928 (2018).
- [22] R. Aaij *et al.* (LHCb Collaboration), *Phys. Rev. Lett.* **119**, 112001 (2017); **121**, 162002 (2018).
- [23] J. Yelton *et al.* (Belle Collaboration), *Phys. Rev. Lett.* **121**, 052003 (2018); M. Sumihama *et al.* (Belle Collaboration), *Phys. Rev. Lett.* **122**, 072501 (2019).
- [24] D. Teodoro *et al.*, *Phys. Lett.* **77B**, 451 (1978).
- [25] S. F. Biagi *et al.*, *Z. Phys. C* **34**, 175 (1987).
- [26] Y. F. Wang, *Int. J. Mod. Phys. A* **21**, 5371 (2006).
- [27] M. Ablikim *et al.* (BESIII Collaboration), *Nucl. Instrum. Methods Phys. Res., Sect. A* **614**, 345 (2010).
- [28] S. Jadach, B. F. L. Ward, and Z. Was, *Comput. Phys. Commun.* **130**, 260 (2000); *Phys. Rev. D* **63**, 113009 (2001).
- [29] R. G. Ping *et al.*, *Chin. Phys. C* **32**, 599 (2008); D. J. Lange, *Nucl. Instrum. Methods Phys. Res., Sect. A* **462**, 152 (2001).
- [30] S. Agostinelli *et al.* (GEANT4 Collaboration), *Nucl. Instrum. Methods Phys. Res., Sect. A* **506**, 250 (2003); J. Allison *et al.*, *IEEE Trans. Nucl. Sci.* **53**, 270 (2006).
- [31] S. Jadach, B. F. L. Ward, and Z. Was, *Phys. Rev. D* **63**, 113009 (2001); R. G. Ping, *Chin. Phys. C* **38**, 083001 (2014).
- [32] S. Actis *et al.*, *Eur. Phys. J. C* **66**, 585 (2010).
- [33] E. Kuraev and V. S. Fadin, *Sov. J. Nucl. Phys.* **41**, 466 (1985).
- [34] Y. S. Zhu, *Chin. Phys. C* **32**, 363 (2008); G. D'Agostini, *Bayesian Reasoning in Data Analysis: A Critical Introduction* (World Scientific, New Jersey, USA, 2003), p. 329.
- [35] A. Sommerfeld, *Ann. Phys. (Berlin)* **403**, 257 (1931).
- [36] C. Tzara, *Nucl. Phys.* **B18**, 246 (1970).
- [37] A. D. Sakharov, *Sov. Phys. Usp.* **34**, 375 (1991).
- [38] M. Ablikim *et al.* (BESIII Collaboration), *Phys. Rev. D* **87**, 032007 (2013); **93**, 072003 (2016); *Phys. Lett. B* **770**, 217 (2017); *Phys. Rev. D* **100**, 051101 (2019).
- [39] M. Ablikim *et al.* (BESIII Collaboration), *Phys. Rev. Lett.* **118**, 092001 (2017).
- [40] L. Maiani, V. Riquer, F. Piccinini, and A. D. Polosa, *Phys. Rev. D* **72**, 031502(R) (2005); X. Liu, X. Q. Zeng, and X. Q. Li, *Phys. Rev. D* **72**, 054023 (2005); S. L. Zhu, *Phys. Lett. B* **625**, 212 (2005).
- [41] F. E. Close and P. R. Page, *Phys. Lett. B* **628**, 215 (2005).